Journal of Operation and Automation in Power Engineering

Vol. 13, No. 1, Jan. 2025, Pages: 74-87

http://joape.uma.ac.ir

Designing a Robust SMC for Voltage and Power Control in Islanded Micro-grid and Simultaneous use of Load Shedding Method

M. Zadehbagheri[*], *M.J. Kiani, S. Khandan*

Department of Electrical Engineering, Yasuj Branch, Islamic Azad University, Yasuj, Iran

Abstract— *Nowadays micro-grids (MG) as one of the most important methods used for electric power generation from renewable energy to reduce dependence on fossil fuels and reducing environmental pollution have been considered. Due to the increasing number of distributed generation (DG) sources and MGs in the power grids, it is of particular importance to design and implement a suitable controller in order to use all the available capacities in these systems. The uncertainty in prediction of power generation can be considered as disturbances into the electrical system, making it difficult to control, and eventually resulting in an unstable system. With the use of power electronic converters the power and voltage of MG can be controlled. In this paper, a 13-bus MG is proposed. This MG includes 3 wind farms and 2 PV farms. A robust sliding mode controller (SMC) is used to control voltage source converters of PV farms. A load shedding program is proposed to avoid complete blackout of MG in case of islanding that recover MG voltage to normal range after a voltage collapse. Simulations were performed using MATLAB/SIMULINK software on a 13-bus IEEE micro grid, and the effectiveness of the proposed control and operational method was investigated and confirmed.*

Keywords—AC/DC converter, DG, Load shedding, Micro-grid, Power control, Robustness, SMC, Voltage control.

1. INTRODUCTION

In recent years, due to the confines of fossil fuels and environmental impacts, more research has been done on distributed generation (DG) systems based on renewable en-ergy sources such as microturbines, fuel cells, photovoltaic systems (PV) and Wind turbines [1]. DG is defined as small, modular generators of electricity located near the point of load of customers. DGs enable the network to reduce the costs of upgrading transmission and distribution systems, while improving the quality and reliability of production capacity without adversely affecting the environment [2, 3]. The units mentioned for DG are generally connected to the main grid via electronic power interfaces. For efficient and optimal connection of DG systems to the existing power network, suitable controllers for electronic power converters should be considered [4].

Since electrical power is generated in DG sources such as DC fuel cells, DC solar cells, and wind turbines as DC voltage and eventually converted to AC voltage by a voltage source inverter (VSI), control of main variables of the network are more necessary. The correct operation of a MG in island mode is specified according to the IEEE 1547.4 standard [5]. In order to comply with the power quality constraints, maintain the balance between production and consumption and prevent excessive overflow of resources in the island mode, the load demand should be proportionally distributed among the micro grid DG units. The implementation of this is usually done by local control of sources and by using active power-frequency (P-w) and reactive power–voltage (Q-E) controllers [6]. Due to the generality of the frequency quantity, the real power is correctly distributed among the sources, and in fact, each source participates in providing the real power of the load according to its capacity. While the relationship between the reactive power and the output voltage range in this controller has made the distribution of this power depends on the impedance of the feeders. Due to the different impedance of the lines of a MG, the conventional Q-E drop characteristic is not able to properly share the reactive power between the sources [7]. In order to solve the problems of MG load shedding caused by the use of conventional dropout characteristics, different solutions have been proposed. In case of choosing the local control method in MG control, achieving the desired control objectives in islanding mode and preventing their interference requires coordination between generation sources. On the other hand, establishing this coordination must be done without the use of a communication channel in order to maintain the advantages of local control. However, due to the small size and less resources of MG and the specific characteristics of MG compared to conventional power grids, it is difficult to achieve a controller that can maintain the stability of the system without using a fast communication channel. In this paper, it is used to control the voltage in the islanded MG using the method of removing the load of the SMC. The sliding mode control method based on changing the control structure has several advantages in comparison with traditional control methods, such as being resistant to parameter changes and external disturbances, as well as good and fast dynamic response. One of the most important disadvantages of the SMC is the error of the reference signal and the controlled signal during the peak time of the controlled voltage waveform. By adapting this controller, the problem is solved and the amount of total harmonic distortion is reduced compared to the usual sliding mode control method.

1.1. Literature review and gap analysis

The performance of renewable energy systems can be improved with proper con-troller design. The use of power electronics converters (inverters) to connect these energies to the power grid

Received: 29 Jun. 2023
Revised: 29 May 2023
Accepted: 16 Jul. 2023
*Corresponding author:
E-mail: mzadehbagheri@gmail.com (M. Zadehbagheri)
DOI: 10.22098/joape.2023.12215.1910
Research Paper

is inevitable. Due to the changes of parameters such as nonlinear components in the converter or inverter, the line and load changes of the electromagnetic interfaces of the converter or inverter deviate from the optimal performance conditions. If the parameter deviation increases, the system will not operate in steady state. Many control methods were used to control and solve the above problem. Therefore, it is nec-essary to choose a precise control strategy that has the best performance under these conditions. Among the various linear and non-linear control methods that have been applied to the power electronics converters so far [8]. As we have already mentioned, the sliding mode nonlinear control method [9] has received much attention due to its unique features such as fast dynamic response, guaranteeing stability, resistance to uncertainty, and simplicity in structure [9]. In SMC, stability is achieved by keeping the system states on a linear sliding surface. In this case, the performance of the system will not depend on the change of parameters and disturbances of the circuit. The MG can include one or more renewable energy sources (RES) such as wind turbines, solar cells and fuel cells, which are used in one of the two modes of islanding or connected to the grid. The smallness of the MG causes the high sensitivity of this system to load changes, which with improper control may cause damage to equipment and resources [10]. Therefore, it is necessary to use a suitable and optimal control system according to the desired conditions [10]. On the other hand, many RES are connected to the MG through power electronics converters. The control of these converters is done by applying the fire command by two different methods. In the first method, the applied signals to the converter switches are directly produced and applied by the corresponding control methods. In the second method, the control system first determines the amount of voltage or reference current of the converter that it must produce, and this signal is applied to the internal control of the converter. The internal control of the converter is done by various methods, including pulse width modulation(PWM). Due to the discrete time nature of power electronics switches, the SMC method can be directly applied to power electronic converters [9] to [11]. One of the most important disadvantages of this method is many changes in the switching mode and chattering phenomenon, which can reduce this phenomenon in the second type. One of the disadvantages of each of these methods is the generation of voltage or current harmonics in the output. Which in any case, according to the IEEE-1547 standard related to the conditions of DG connection to the grid, should not exceed 5% in the distribution voltage. Many methods for controlling the inverter output voltage and power management have been presented in recent years, and many researchers are working on the controller design to control AC/DC power electronics converters. In [12], a control scheme based on the transfer function in nominal conditions for a DG unit in islanding mode is stated that this control method is suitable for balanced and predetermined loads, but it does not cover many load changes. In [13], a robust control method for balanced and unbalanced systems was proposed and investigated by considering the uncertainty of load parameters, but nevertheless, nonlinear loads have not been fully investigated. In [13, 14], methods based on PI controller have been reviewed. A control strategy for a three-phase single-phase photovoltaic (PV) system connected to the distribution network proposed in [14]. The proposed control strategy uses an internal current control loop and an external DC link voltage control loop. The current control loop allows the dc link voltage to be regulated and provides power factor control, and the voltage control loop specifically separates the dynamics of the PV system from the distribution network and loads. The dc link voltage control scheme provides control and maximization of the actual power output of the PV system. In [14] and [15], SMC is used to control the power electronics converter and to determine the reference active power from the output voltage and DC output current at certain slip levels. However, there is no mention of the chattering phenomenon and the topics of time delays. The SMC method based on changing the control structure has several advantages in comparison with traditional control methods, including being resistant to parameter changes and external disturbances, as well as good and fast dynamic response [16] and [17]. In [18], a first-order sliding mode controller is used to adjust the active and reactive output power of a PV system. In this indication, an effective control strategy for a three-phase PV system that provides local load and is also connected to the network is proposed. The maximum power is obtained by the internal current control loop and the external voltage control loop. The PV output is built by a dc / ac voltage source converter. But the systems of this converter are highly nonlinear and coupled as traditional PI controllers do not provide satisfactory performance for operation change conditions and load change uncertainty, feedback linearization scheme has been used. Sliding mode control technique is used to work with linear feedback control to solve the problem of uncertainty and add resistance to the control algorithm. A flexible control structure that can be operated in both network and islanded states without the need for an island detection mechanism suggests in [19]. A distributed method is presented in [20] to solve OPF in the tertiary level. The method considers the impact of droop parameters and the load model on power loss and provides a satisfactory response to the unbalanced load. A distributed heuristic method based on backward and forward procedures is proposed in [20]. The distributed heuristic method minimizes power loss in the backward procedure and then updates voltages using the distributed protocol in the forward procedure. The method is able to solve the distributed OPF in an islanded MG with a balanced load. The secondary level is completely removed from the hierarchical control of the MG in methods proposed in [21]. These methods that are proposed to solve the OPF in the tertiary level could not take the responsibility of the secondary level because the time horizon of the tertiary level is too long compared with the secondary level. For example, 5 minutes is considered as scheduling time for the tertiary control in [22], but it is not acceptable. Some loads may change before the tertiary levels' time horizon, and both frequency and voltage change due to the primary controller's response. In addition, sometimes, operators give a high priority to nominal conditions as opposed to the optimal operation owing to the presence of critical loads with special power quality features, and the secondary controller is in charge of nominal conditions. The secondary has also a faster response time. Since the computation time of the controllers is not comparable with that of complicated optimization processes, the presence of the secondary level is necessary for most applications. In [22], the authors proposed the use of SMC to achieve MPP based on maximizing the PV cell power relation This method does not use the solar array current sensor. The solar array current information is obtained from the sliding mode observer and injected into the maximum power point tracker (MPPT) to generate the voltage reference. In [23], the dynamics of the microgrid in the island mode has been investigated. It is assumed that the microgrid consists of an inverter distributed generation source and a load. DG model includes DC voltage source, power electronic converter, transformer and filter. In the working mode connected to the grid, the traditional control of active and reactive power is applied to the converter. This control becomes unstable if it goes to the island mode due to the imbalance of production and consumption powers. Therefore, if islanding is detected, a new controller is introduced to control the voltage. In [24], in order to reduce the reactive power sharing error caused by the impedance difference of the feeder, by using the current feedback loop, the output of the DG units is equipped with a virtual inductor impedance. In this way, the voltage drop resulting from the output in the controller of all units will be the same. The use of the virtual impedance method can also lead to the reduction of the reactive power sharing error by correcting the slope of the drop characteristics. In [25], secondary frequency control is used on the converter of renewable energy sources to control the load frequency. One of the appropriate controllers to consider various uncertainties in a system

is predictive control, which has the ability to predict future events and adopt appropriate control actions. Also, in [26], a method for providing coordinated control of wind turbine blades and hybrid electric vehicles, based on predictive control, in order to reduce power and frequency fluctuations in the microgrid is presented. In [27], another example of microgrid modeling is presented. The control strategy for dividing the load between DGs by maintaining the quality of voltage, current and power in two modes connected to the grid and islanded is discussed. The important point in this model is that each DG feeds a load that can be unbalanced or non-linear. Of course, this is if the DGs are converters. Another point in this model is the assumption of grid robustness and as a result the voltage angle drop, reactive power and active voltage power size to work in island mode. In [28], an adaptive load shedding method for an industrial network has been proposed with the help of a neural network, in which transient stability analysis has been used for better training of the network, to reduce the load shedding. For this purpose, dynamic system models have been used. Production power, consumption power, frequency change rate before network isolation and frequency change rate after network isolation are considered as input variables and the optimal amount of load elimination is considered as output variable.

1.2. The purpose of the research and its importance

These days, due to the destructive effect of fossil fuels and greenhouse gases, the use of renewable energies such as solar and wind energy are increasing. The performance of renewable energy systems can be improved by proper controller design. It is inevitable to use power electronics converters (inverters) to connect these energies to the power grid. Due to the changes of parameters such as nonlinear components in the converter or inverter, the line and load changes of the electromagnetic interfaces of the converter or inverter are deviated from the desired performance conditions. If the deviation of parameters increases, the system will not work in stable. Many control methods were used to control and solve the above problem. Therefore, it is necessary to choose a precise control strategy that has the best performance under these conditions. This paper aims to implement the sliding mode controller on the inverters connected to the MG. These inverters should control the operation of the renewable resources present in the MG in two working modes connected to the grid and islanding.

1.3. Contributions and outline

Nowadays, the use of MGs is considered as one of the important methods of using renewable energy to reduce the dependence of electric power generation on fossil fuels and reduce environmental pollution. With the increase in the use of MGs and the advancement of related technologies, the issue of MGs management in grid-connected and islanded modes is very important. Similar to conventional systems, it is essential to have an acceptable voltage and frequency in a MG. In this paper, considering the unintentional random islanding condition, a robust controller is designed to stabilize the MG performance during the islanding mode. Also, load shedding method is presented as one of the last measures to prevent system shutdown. The proposed control system facilitates the desired power exchange between grid-connected and islanding MGs and achieves effective voltage and frequency regulation in the MG system. In the state of being connected to the grid, the DG sources produce the specified powers well and deliver them to the MG. The main grid is responsible for resolving the power imbalance and maintaining the MG voltage. In this paper, after islanding mode, the voltage of the MG dropped sharply due to power imbalance. By removing parts of the less important loads, the network voltage was maintained and the rest of the loads were fed well. The most significant contributions of this article are listed as follows. Using error dynamics, proposed sliding mode surfaces to provide more stable motion for converter-based mode variables under parameters

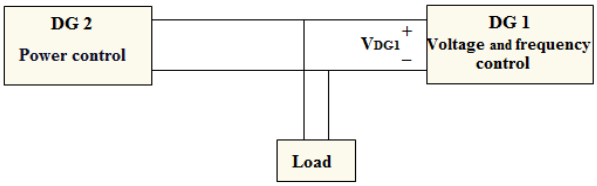

Fig. 1. Diagram of a MG with two DG units

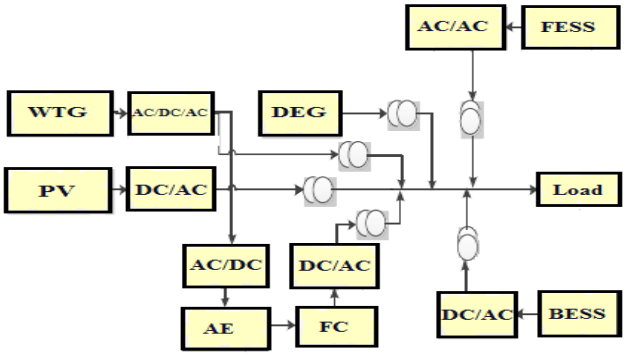

Fig. 2. Schematic of MG

changes are defined as the contribution of this paper-A new robust scheduling model is developed for islanded MGs to withstand the negative effects of unexpected events-Due to the uncertainty in the occurrence time and duration of the unintentional islanding mode, a robust SMC was implemented on the DC/AC converters connected to the MG to ensure the reliability of the system and restore the system to normal operation after fixing the fault.

2. DYNAMIC MODEL OF SYSTEM

2.1. MG configuration

Fig. 1 shows a microgrid with two production units in island mode. According to the block diagram in Fig. 2 each unit of renewable energy sources can include wind turbines, solar cells, fuel cells, etc. According to this figure, every microgrid includes four main parts of the energy source, ac/dc power inverter for wind turbines or ac/dc converters for fuel cells and solar cells. The dc/ac inverter and the LC output filter are intended to eliminate the harmonic components of the output voltage that provides power to local loads.

Fig. 2 shows the schematic of the studied MG, which is separate from the main grid. The used MG includes a photovoltaic (PV), a conventional diesel engine generator (DEG), a wind turbine generator (WTG), a fuel cell (FC), two energy storage sources including a battery (BESS), a flywheel (FESS) and it is an aqua electrolyzer (AE). The energy sources used in the MG are connected to the main bus with power electronic converters and their injection power to the main bus is controlled from this converter [30].

2.2. Modeling of MG

The general figure of the MG studied in this paper is shown in Fig. 3. The topology of this MG is based on the IEEE 13-bus distribution network, which loads and distributed generation sources are set according to the appropriate conditions for investigation in this paper [31].

This MG includes a distribution substation, 12 buses, 10 lines and 7 loads. Loads consist of a combination of constant impedance

Table 1. Taxonomy of related research works

References	Uncertainty Modeling	Load Priority	DRP	Solution Method
[11]	SP	–	Yes	Multi objective compromised program method
[12]	SP	–	Yes	Bat algorithm
[15, 17]	SP	Yes	–	MILP Solver
[20]	Robust model predictive control	Yes	Yes	model predictive control (MPC)-PI
[23]	Robust optimization	–	Yes	ST-SMC
[25, 40]	Robust optimization	Yes	Yes	Hybrid GA–MILP
[29]	Robust model predictive control	–	Yes	Metaheuristic algorithms
[34]	EMHA	–	Yes	GWO
[35]	Adaptive robust optimization	Yes	Yes	column and constraint generation (C&CG) algorithm
[36]	Optimal UVLS method.	Yes	Yes	HDCEMA-PSO-WOA
[37]	Unified robust hierarchical control	–	Yes	ABINFTSMC
Current paper	Robust optimization	Yes	Yes	SMC

DRP: demand response program
MOCPM: Multi-objective compromised program method
HDCEMA: hybrid discrete continuous exchange market algorithm
ABINFTSMC: adaptive back stepping integral nonsingular fast terminal sliding mode control
ASMC: adaptive sliding mode controller
UVLS: under-voltage load shedding
UFLS: under frequency load shedding
EMHA: entropy method with high adaptability
MILP: mixed-integer linear programming
ST: super twisting
WOA: whale optimization algorithm
GWO: grey wolf optimizer
SP: stochastic programming

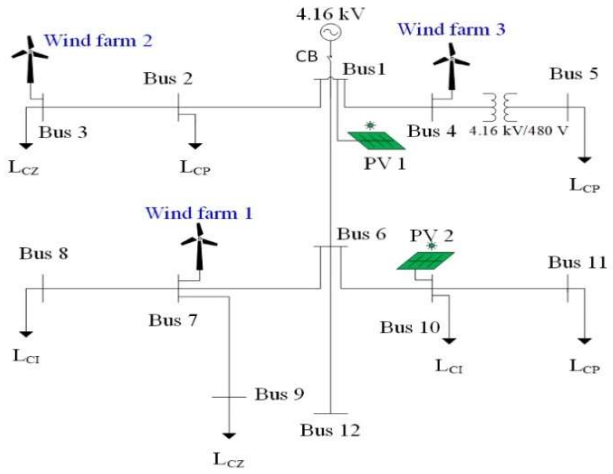

Fig. 3. Proposed MG

(LCZ), constant current (LCI) and constant power (LCP) loads. The distribution substation voltage is 4.16 kV. There is a transformer between buses 4 and 5 that step down the voltage from 4.16 kV to 480 V. The system consists of three wind farms located in 7, 3, and 4 buses. Also, there are two PV systems in this network, which are located in buses 1 and 10. Since in this paper there is no focus on demand side management and generation planning of generators, the demand of loads and available power of DGs are considered fixed.

2.3. PV Model

A solar cell is the main component of a solar panel. A photovoltaic module is formed by connecting a large number of solar cells in series and parallel. A single solar cell can be modeled as a current source with a diode and two resistors. (Fig. 4)

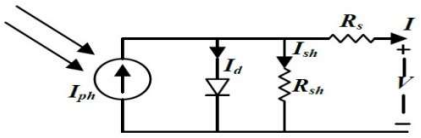

Fig. 4. Single diode model for solar cell

Solar cell efficiency is very low. In order to increase the efficiency, methods are used to correctly match the load and the source. One of these methods is maximum power point tracking (MPPT).

A) Three-phase PV system model connected to the grid

The state space model of the three-phase network-connected photovoltaic system shown in Fig. 5 can be obtained with the dynamic equation described below [32]:

$$\begin{aligned} v_a - e_a &= Ri_a + L\frac{di_a}{dt} \\ v_b - e_b &= Ri_b + L\frac{di_b}{dt} \\ v_c - e_c &= Ri_c + L\frac{di_c}{dt} \end{aligned} \tag{1}$$

Depending on the condition of the switches and the output voltage of the solar array, this equation can be written as follows:

$$\begin{aligned} \dot{i}_a &= -\frac{R}{L}i_a - \frac{1}{L}e_a + m\frac{v_{sa}}{L} + \Delta d_a \\ \dot{i}_b &= -\frac{R}{L}i_b - \frac{1}{L}e_b + m\frac{v_{sb}}{L} + \Delta d_b \\ \dot{i}_c &= -\frac{R}{L}i_c - \frac{1}{L}e_c + m\frac{v_{sc}}{L} + \Delta d_c \\ \dot{v}_{sa} &= -\frac{1}{C}i_{sa} - \frac{1}{C}(i_a - i_b - i_c) + \Delta d_{sa} \end{aligned} \tag{2}$$

Where, Δd are the uncertainties of the system [32].

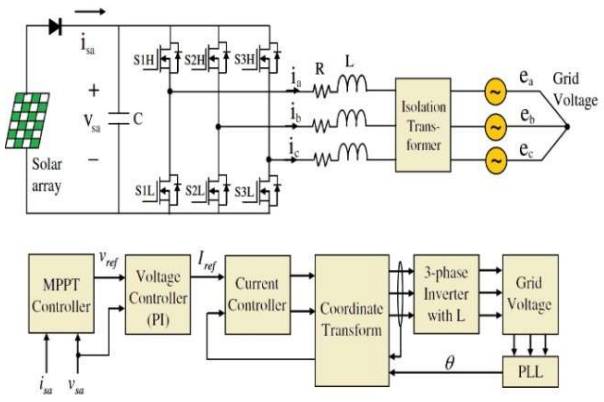

Fig. 5. Structure of three-phase network-connected PV system [32]

This model is nonlinear and variable with time, but by converting equation (2) using the angular frequency of the rotating reference frame which is synchronized with the mains line voltage and the d-axis of the source phase voltage is zero, the model is invariant with time but nonlinear equation (4) is obtained [33]. The transfer matrix K_{abc}^{qd} is as follows:

$$K_{abc}^{qd}=\frac{2}{3}\begin{pmatrix} cos\theta & \cos(\theta-120^{\circ}) & \cos(\theta+120^{\circ}) \\ sin\theta & \sin(\theta-120^{\circ}) & \sin(\theta+120^{\circ}) \\ 1/2 & 1/2 & 1/2 \end{pmatrix} \quad (3)$$

Using the above conversion matrix and performing the dq conversion, equation (2) can be written as follows: [24].

$$\frac{d}{dt}\begin{bmatrix} i_d \\ i_q \\ v_{sa} \end{bmatrix}=\begin{bmatrix} -\frac{R}{L} & w & \frac{1}{L} \\ -w & -\frac{R}{L} & \frac{1}{L} \\ -\frac{1}{C} & -\frac{1}{C} & 0 \end{bmatrix}\begin{bmatrix} i_d \\ i_q \\ v_{sa} \end{bmatrix}$$

$$+\begin{bmatrix} -\frac{1}{L} & 0 & 0 \\ 0 & -\frac{1}{L} & 0 \\ 0 & 0 & \frac{1}{C} \end{bmatrix}\begin{bmatrix} e_d \\ e_q \\ i_{sa} \end{bmatrix}+\begin{bmatrix} \Delta d_d \\ \Delta d_q \\ \Delta d_{sa} \end{bmatrix} \quad (4)$$

Where,

$$i_{qd}=K_{abc}^{qd}.i_{abc}, \quad e_{qd}=K_{abc}^{qd}.e_{abc}, \quad S_{qd}=K_{abc}^{qd}.S_{abc}$$

The power that delivered to the grid is equal to:

$$\begin{aligned} S&=P+jQ \\ P&=\frac{3}{2}(e_d i_d+e_q i_q) \\ Q&=\frac{3}{2}(e_q i_d-e_d i_q) \end{aligned} \quad (5)$$

Where, P and Q are active and reactive power, respectively. These capabilities can be written as a matrix:

$$\begin{bmatrix} P \\ Q \end{bmatrix}=\frac{3}{2}\begin{bmatrix} e_d & e_q \\ e_q & -e_d \end{bmatrix}\begin{bmatrix} i_d \\ i_q \end{bmatrix} \quad (6)$$

According to the above relation, if we assume the total voltage along the q-axis (i.e., $e_d=0$ is considered), the active and reactive powers can be decoupled from each other and written as follows:

$$\begin{aligned} P&=\frac{3}{2}e_q i_q \\ Q&=\frac{3}{2}e_q i_d \end{aligned} \quad (7)$$

And with this assumption, the active power is controlled by i_q current and the reactive power is controlled by i_d current.

3. PROPOSED CONTROLLER DESIGN

3.1. Design of SMC

The SMC method is a control technique based on variable structure systems that follows a series of rules to improve system behavior, including response speed, stability and system resistance. SMC design can be divided into two subsections. Designing a stable level and designing a control law to drive the system states to the selected level in a limited time. The design of the surface should take into account all the limitations and required features, so it should be optimally designed to meet all the conditions. Sliding mode controller design starts from sliding surface design. The sliding surface is usually obtained from the linear error composition of the state variables, which is the difference between the state variables and their reference values. Therefore, in this case, the sliding surface can be designed using solar array voltage and inductor current errors in a three-phase network-connected photovoltaic system. The reference voltage of the solar array is the DC voltage generated by the MPPT, but the voltage of the solar array fluctuates due to mismatch between the parameters, which causes the sliding mode to malfunction. The main purpose of the photovoltaic system connected to the grid is to transfer the maximum power of the solar cell to the grid [34]. As a result, the sliding surface must be designed to control the inductor current and power of the solar array simultaneously. This goal can be achieved by selecting the sliding surface using the inductor current error. If the reference inductor current is expressed as a function of the solar array power, then the sliding surface can control the inductor current and thus the solar array power. By ignoring the losses between the solar array and the grid and zeroing the reactive power control by setting, $i_{dref}=0$, the following equation is obtained from equation (7).

$$P_{sa}=P_{grid}=\frac{3}{2}e_q i_q \quad (8)$$

The proposed integral sliding surface will be as follows [16, 17]:

$$\begin{aligned} \sigma_1&=i_{dref}-i_d+c_1\int_0^t(i_{dref}-i_d)\,dt \\ \sigma_2&=i_{qref}-i_q+c_2\int_0^t(i_{qref}-i_q)\,dt \end{aligned} \quad (9)$$

Which,

$$i_{qref}=\frac{2}{3}\frac{P_{sa}}{e_q}=\frac{2}{3}\frac{P_{ref}}{e_q}, \quad i_{dref}=0$$

P_{ref}, is the reference power of the solar array specified by the MPPT controller. The next step is to design a control input to satisfy the condition of sliding mode, which is obtained by zeroing the sliding surface and its derivative in equations (3). The control input has the following structure:

$$\begin{aligned} v_d&=v_{d_{eq}}+v_{nd} \\ v_q&=v_{q_{eq}}+v_{nq} \end{aligned} \quad (10)$$

Veq is the equivalent control input that determines the behavior of the system on the sliding surface and v_{ni} is the nonlinear switching input that directs the state variable to the sliding surface and keeps the variable on the sliding surface in the event of changes in parameters and perturbations. The equivalent control input is obtained from the immutability condition and is specified as follows [35]:

$$\sigma_i=0 \quad and \quad \dot{\sigma}_i=0 \rightarrow v_i=v_{eq} \quad (11)$$

In summary, the control input is equivalent to the following [35, 36]:

$$\begin{aligned} v_{d_{eq}}&=Ri_d-wLi_q+e_d+c_1L(i_{dref}-i_d) \\ v_{q_{eq}}&=Ri_q+wLi_d+e_q+c_1L(i_{qref}-i_q) \end{aligned} \quad (12)$$

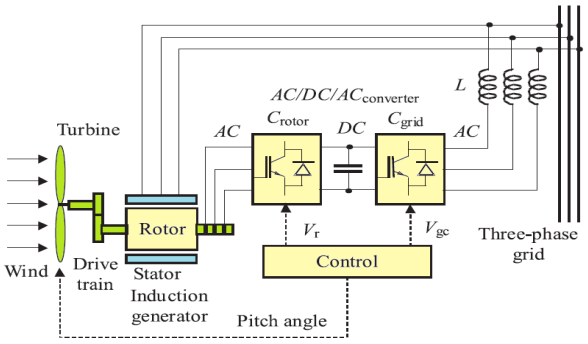

Fig. 6. Wind turbine system and DFIG [37]

Discontinuous switching input can be selected as follows:

$$v_{nd}=k_1.sgn(\sigma_1) \quad v_{nq}=k_2.sgn(\sigma_2) \tag{13}$$

If the equations (12) and (13) are placed in equations (10), the range k_i which leads to the establishment of $\sigma_i\dot{\sigma}_i < 0$, is defined as follows [36]:

$$\begin{aligned}
&\sigma_1\dot{\sigma}_1<0\\
&\sigma_1\left(\frac{R}{L}i_d-wi_q+\frac{e_d}{L}+c_1\left(i_{dref}-i_d\right)-\Delta d_d\right.\\
&\left.-\frac{1}{L}\left(Ri_d-wLi_q+e_d+c_1L\left(i_{dref}-i_d\right)+k_1sgn\left(\sigma_1\right)\right)\right)<0\\
&\sigma_1\left(-\frac{k_1}{L}sgn\left(\sigma_1\right)-\Delta d_d\right)<0\\
&\sigma_2\dot{\sigma}_2<0\\
&\sigma_2\left(\frac{R}{L}i_q-wi_d+\frac{e_q}{L}+c_2\left(i_{dref}-i_q\right)-\Delta d_q\right.\\
&\left.-\frac{1}{L}\left(Ri_q-wLi_d+e_q+c_2L\left(i_{qref}-i_q\right)+k_2sgn\left(\sigma_2\right)\right)\right)<0\\
&\sigma_2\left(-\frac{k_2}{L}sgn\left(\sigma_2\right)-\Delta d_q\right)<0
\end{aligned} \tag{14}$$

As a result, the range of switching benefits is as follows:

$$\begin{aligned}
k_1 &> L\left|-\Delta d_d\right|\\
k_2 &> L\left|-\Delta d_q\right|
\end{aligned} \tag{15}$$

According to the equations (12),(13) and (15), the control inputs $v_i = v_{eq} + v_{ni}$ are as follows [18]:

$$\begin{aligned}
v_d&=Ri_d-wLi_q+e_d+c_1L\left(i_{dref}-i_d\right)+k_1\cdot sgn\left(\sigma_1\right)\\
v_q&=Ri_q+wLi_d+e_q+c_2L\left(i_{qref}-i_q\right)+k_2\cdot sgn\left(\sigma_2\right)\\
k_1&=k_2=1 \quad c_1=c_2=1000
\end{aligned} \tag{16}$$

3.2. Wind turbine model

Fig. 6 shows a wind turbine with a dual-feed induction generator (DFIG). The AC/DC/AC converter is divided into two parts: Converter on the rotor side (Crotor) and converter on the grid side (Cgrid). Crotor and Cgrid are voltage source converters that use forced commutation power electronics (IGBT) to convert DC voltage to AC voltage. The control system generates pitch angle command signals and voltages Vr and Vgc respectively for Crotor and Cgrid in order to control wind turbine power, DC bus voltage and reactive power or grid terminal voltage.

Rotor side converter to control the power of the wind turbine and the measured voltage of the network terminals is used. The Cgrid converter is used to adjust the DC bus capacitor voltage. In addition, in this model, it is allowed to use the Cgrid converter to generate and absorb reactive power.

4. LOAD SHEDDING

Usually, the MG is connected to the national grid and exchanges power with it. DGs are expected to produce a specified power, for example to minimize network losses. This is different in different systems [38]. In this way, the network can act as a backup and solve the power imbalance of the MG. Micro grid islanding happens either planned or sudden. In the transition mode from the network-connected state to the islanded state, the MG tries to stay on its previous condition, but it is practically impossible, and in order to maintain stability, it is necessary to remove some of the load. MG usually receives power from the main network when connected to the network. Therefore, in the case of islanding, power will be unbalanced [38]. For this purpose, a method for the stability of the isolated MG will be presented below. As with traditional systems, disconnected MG can cause a variety of events, such as generator outages, power-consumption imbalances, and power quality problems. Therefore, the safe operation of MG requires proper control. Different local, general, secondary and emergency control loops are used to maintain the MG [39, 40]. The main purpose of controllers is to ensure system reliability and restore normal operation after a disturbance, but each controller has the ability to respond to some disturbances [41]. Small disturbances do not require critical action, but large disturbances require emergency control to prevent the system from shutting down. In this article, load shedding is considered as one of the emergency methods. Emergency control can occur in both supply and demand. The load shedding strategy is related to the demand side. In this method, some loads are cut so that the available production can supply the remaining loads [42]. In the strategy used in this paper, at first less important loads and then, with a certain strategy, more important loads are prioritized for elimination, which are based on the voltage signals received from the load bases. The load shedding method is illustrated in Fig. 7. The first step will be to determine all the necessary parameters of the system, including the parameters of loads and generators. Then the operation mode of the system will be considered as well. The next step is to calculate the frequency droop and then adjust the primary and secondary power if necessary. After that, the minimum amount of load shedding and the amount of load shed at each bus will be determined by the optimization algorithm. After the amount of load shed is calculated, the load shedding process will be operated. And finally, the overall check must be processed to ensure the system is safe and secure [9].

4.1. Load shedding standards for MG

As it was stated, different standards and methods are used for load shedding. Load shedding methods are divided into two categories: frequency and voltage methods. Frequency load shedding is the most common method of load shedding and the rate of frequency changes is its most widely used criterion [41]. In addition, during a major disturbance in the system, in addition to the lack of active power, reactive power is also reduced, voltage and frequency stability is endangered. Therefore, combined load shedding according to frequency and voltage standards is a suitable solution for providing an effective method of load shedding. According to the technical situation governing the MG, it is essential to pay attention to the following two points in determining the load shedding criteria: – In the MG, due to the low and variable inertia caused by the presence of scattered production sources, including the wind power plant, the frequency fluctuations will be more – In the MG, due to the proximity of production and load in the low-pressure and medium-pressure system, the electrical distance between the busses is short. Considering these two points, it is inappropriate to use the df/dt criterion in a system where there is a wind power plant. Also, the production rate of the wind power plant, which is caused by the wind speed, affects the frequency behavior of the MG, and the lower the inertia of the system, the greater this effect will be. On the

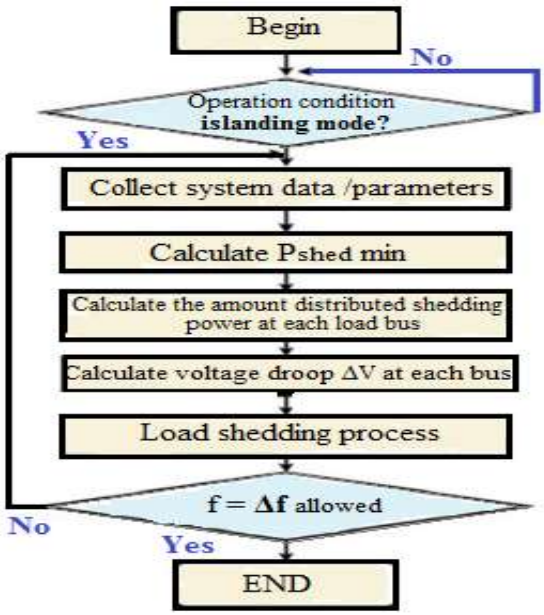

Fig. 7. Proposed load shedding method

other hand, some combined heat and power (CHP) units are cut off due to the bad performance of the water and oil pump due to the voltage fluctuation caused by the error. Therefore, adding the voltage criterion along with the frequency criterion helps the stability of the system as much as possible. According to these points, frequency, voltage and wind speed, they will be suitable criteria for load shedding in the MG [42].

4.2. Adjustment of load shedding steps

Load shedding is basically done in several stages. The entire load that must be removed during the different stages of load shedding is determined based on the worst foreseeable case and considering the maximum amount of production loss in the network. The number of stages and the elimination load related to each stage should be selected appropriately. In case of improper setting of frequencies and the amount of elimination load in each stage, unpleasant consequences such as load shedding in the initial stages and creation of excess frequency or low load shedding in the initial stages and severe frequency drop are unavoidable. In case of a drastic decrease in frequency, the frequency protection relays of the generating units give a trip command, which leads to widespread shutdowns [40]. In general, there are no specific rules for setting frequency load shedding steps, which include the number of steps and the loading threshold frequency. The selection of these parameters strongly depends on the structural and technical conditions of the studied system and its transient stability analysis. At the same time, we try to observe the following general principles for the regulations in question. In general, the implementation of load shedding in the number of more stages and less removal load in each stage is priority over the load shedding in the number of fewer stages and more removal load related to each stage. For this reason, it is better to set the load shedding frequencies of the frequency relays not too close to each other, but have a logical distance. Compliance with this issue is due to the practical time delay related to the relays and the operation of the keys, and it is necessary to avoid interference between load shedding stages. Based on the studies that have been done so far, the load shedding is based on the following three different plans: – The total elimination load as well as the amount of elimination load in each stage is fixed; – The load of removal is fixed, but the load that is removed at each stage is variable; – The total elimination load as well as the load of each stage changes according to the amount of frequency reduction. The third method has a higher priority due to its higher flexibility and the possibility of carrying out load shedding based on the intensity of the disturbance [42, 43].

Table 2. Active power demand and supply

BUS	Generated Active Power (MW)	Active Load Demand(MW)
1	0.4	0
2	0	2
3	1.5	3
4	1.5	0
5	0	1
6	0	0
7	6	0
8	0	5
9	0	4
10	0.4	3
11	0	4
12	0	0

5. RESULTS AND DISCUSSIONS

The MG simulation shown in Fig. 3 was performed in MATLAB Simulink environment. This MG has 5 sources of distributed generation. These resources include 2 solar farms and 3 wind farms. The circuit breaker between bus 1 and the distribution substation has the task of changing the state of the micro grid to the island and connected to the network. Information about the production capacities and loads of this micro grid is given in Table 2. As shown in Fig. 2 the bars are often divided into four sections, each of which is 0.25 per unit. These loads are divided into four categories based on their importance, which will be fully examined in the load shedding simulation section.

In this simulation, there are two PV fields, each of which consists of 4 PV arrays, each of which delivers a maximum power of 100 KW at 1000 w/m^2 of solar radiation (Fig. 8) .Each solar array consists of 64 parallel strands with 5 series modules in each strand. The amount of sun-light for each of the 4 arrays is 1000 w/m^2 and the surface temperature of the arrays is 40, 44, 35 and 45, respectively. Each PV array is connected to a DC/DC amplifier converter. The output of these converters is connected to a common 500 V DC bus. Each increment converter is controlled separately by MPPT. MPPTs use the P&O method to get the most power possible. A three-phase voltage source converter converts 500 V DC voltages to 260 V AC voltages. A 260V/4.16KV three-phase transformer with a capacity of 400 kVA is used to connect the converter to the MG.

Fig. 9 shows the general structure of the PV converter controller system. This structure consists of MPPT controller, sliding mode controller and pulse width modulation generator. The MPPT controller uses the array current and voltage to track the maximum power point. The sliding mode controller controls the inductor current using the sliding surface to follow the reference current. The PWM manufacturer produces the switching pattern according to the control input. Fig. 10 shows the SMC block in the Simulink environment. The inputs of this block include reference currents, currents measured after conversion to dq, and voltages measured in the dq frame. The outputs of this block are control inputs that are used to generate converter pulses.

Fig. 11 shows the blocks that build up the sliding mode controller. These block diagrams are the result of implementing

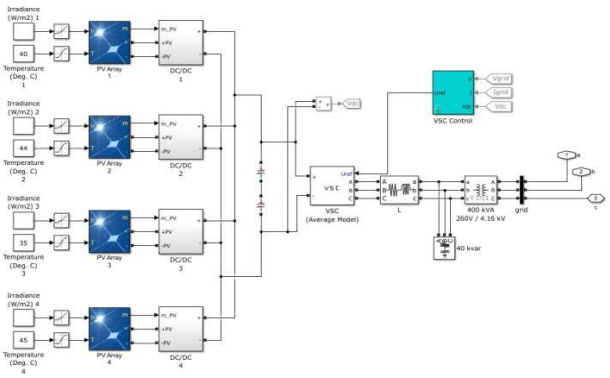

Fig. 8. Simulation of Solar Farm in Simulink Environment

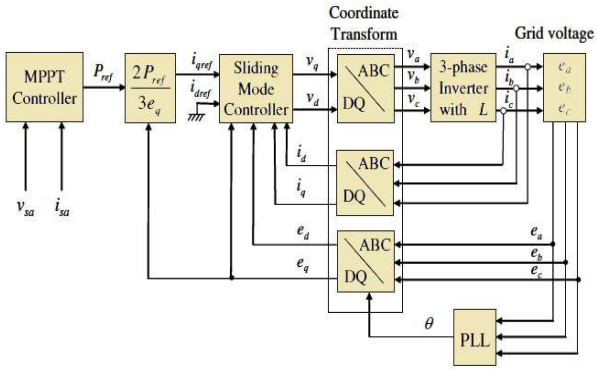

Fig. 9. General Structure of the PV system converter controller

equation (7) and (15). Fig. 11a shows how to create σ_1 and vd, and Fig. 11b shows how to create σ_2 and vq.

Fig. 12 shows the output power of one of the PV systems connected to the grid.

In this case, PV injects active power of 350KW to the MG. Reactive power is zero. It should be noted that both PVs in the MG show the same performance. In this MG, there are two wind farms with a power of 1.5 MW and one wind farm with a power of 6 MW. Each of the 1.5 MW farms includes three 0.5 MW wind turbines. The 6MW farm consists of four, 1.5MW turbines. Wind turbines consist of doubly fed induction generator (DFIG), which consists of a wound-rotor induction generator and an AC/DC/AC converter. The stator winding is connected to a 575V bus, which is connected to the MG through a 575V/4.16KV transformer. DFIG technology allows extracting the most wind energy at low wind speeds by optimizing the turbine speed and minimizes the

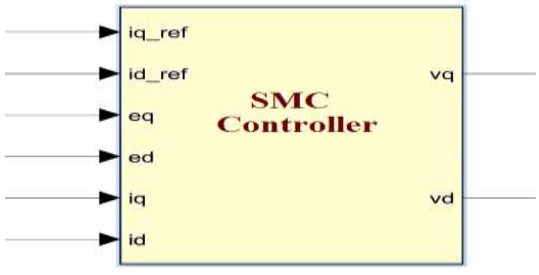

Fig. 10. SMC controller block in Simulink environment

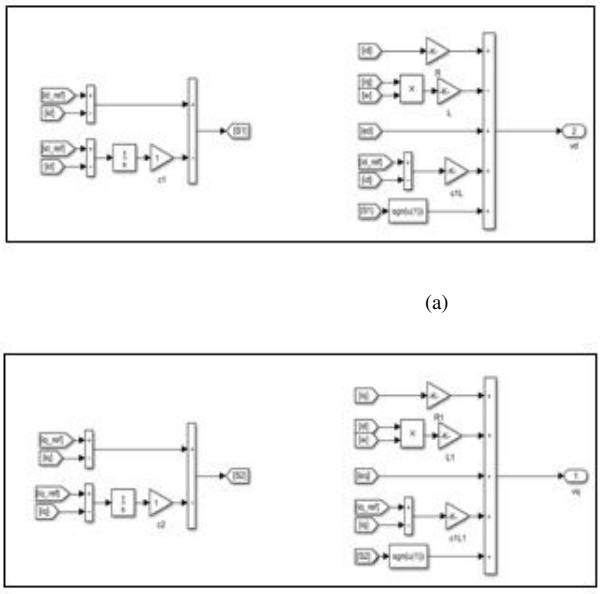

(a)

(b)

Fig. 11. Simulated Sliding Mode Controller: (a) shows how to create σ_1 and v_d; (b) shows how to create σ_2 and v_q.

Fig. 12. Output power of PV, bus 1 in grid connected state

mechanical stress on the turbine during strong winds. In this simulation, the wind speed is considered constant at 15 meters per second. The control system uses a torque controller to keep the speed at 1.2 Pu. The generated reactive power is set to zero. Fig. 14 shows the active power of the 6 MW wind farm.

Considering that the total load is equal to 22 MW and the total production capacity of renewable resources in the MG is 9.8 MW, the main grid establishes the power balance in the MG by providing the remaining required power. By injecting 12 MW of power into the MG, the main grid balances the power in this MG.

5.1. Checking faults in the MG

Two-phase to ground faults have been investigated on the proposed MG in grid-connected mode. This fault will be checked on bus number 9. In this case, two phases a, and b are connected through a 1 milliohm fault resistor. This error occurs in 0.2 seconds and will remain in the network for 1ms.The figure of the busses current changes in this case will be as Fig. 15 and Fig. 16.

After checking the fault on bus 9 of the MG, the controllers were able to control the disturbances in less than 0.05 seconds and return the network to its permanent state.

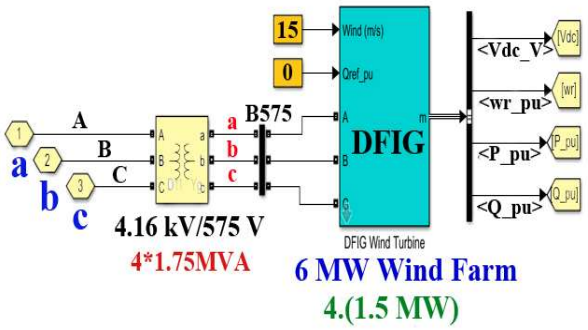

Fig. 13. Block diagram of wind farm in Simulink environment

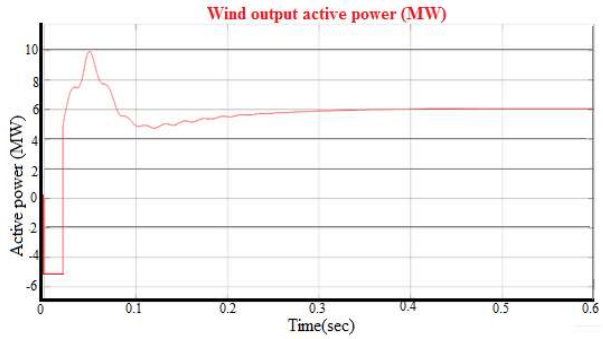

Fig. 14. The output active power of the wind farm 6 MW

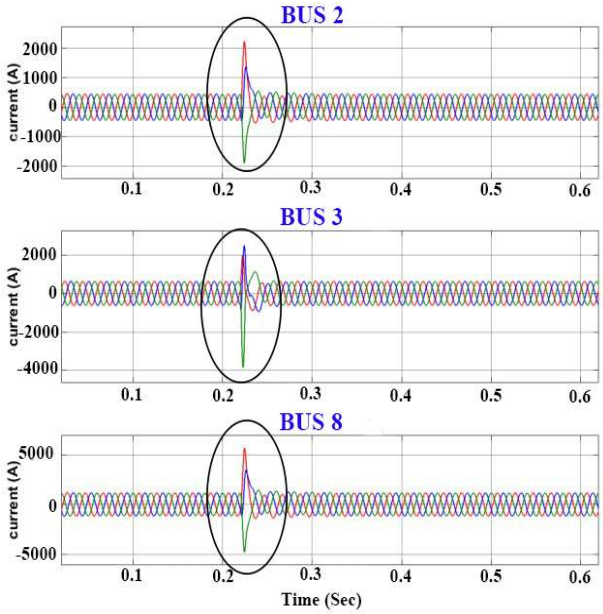

Fig. 15. Changing the buses current in a two-phase to ground fault (Buses 2, 3, 8)

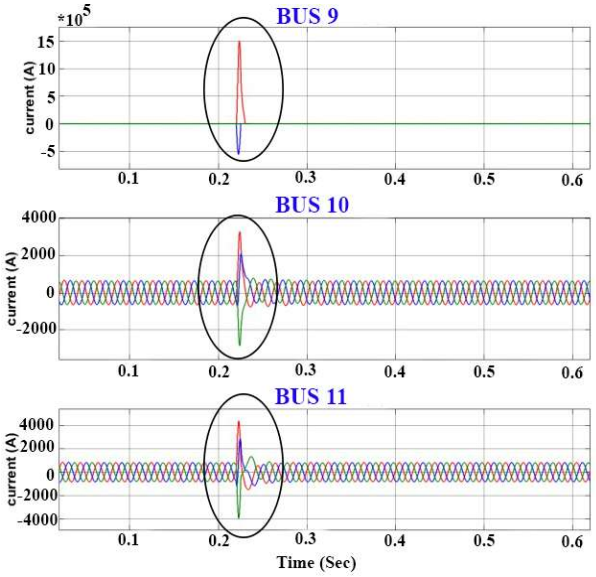

Fig. 16. Changing the buses current in a two-phase to ground fault (Buses 9, 10, 11)

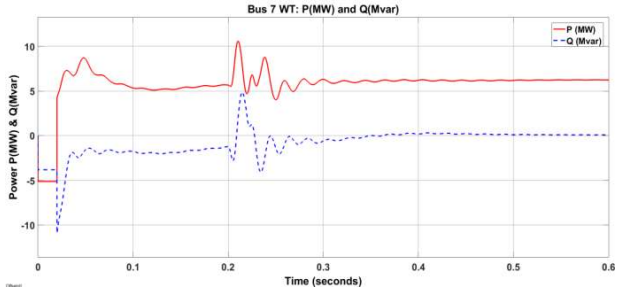

Fig. 17. Output power of bus 7 wind turbine during two-phase to ground fault

5.2. Islanded MG

In 0.2 seconds, the MG goes into island mode when the breaker located at the point of common coupling (PCC) is opened. In the island mode, wind turbines generate reactive power by changing the adjustment point. In this case, distributed generation sources are able to supply about 45% of MG loads. Since the load demand exceeds the production capacity and wind turbines are able to produce limited reactive power, voltage collapse occurs.

Fig. 19 shows the busses voltage after the main grid is disconnected and the MG is islanded. As can be seen in this figure,

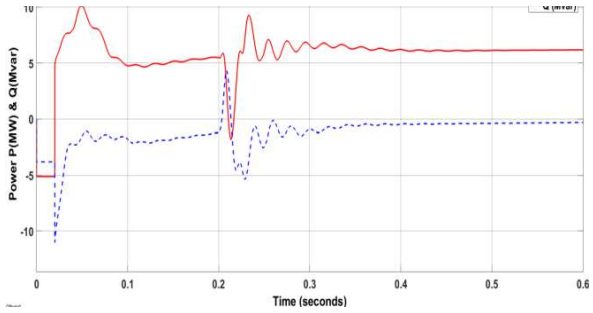

Fig. 18. Bus 7 PV output power during three-phase to ground fault

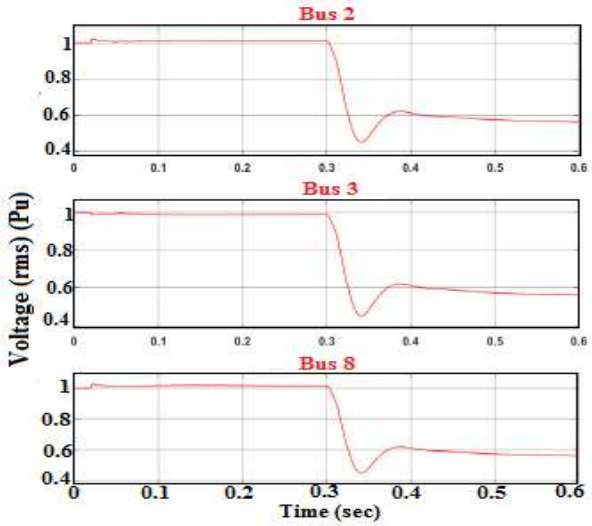

Fig. 19. Voltage collapse in islanding mode

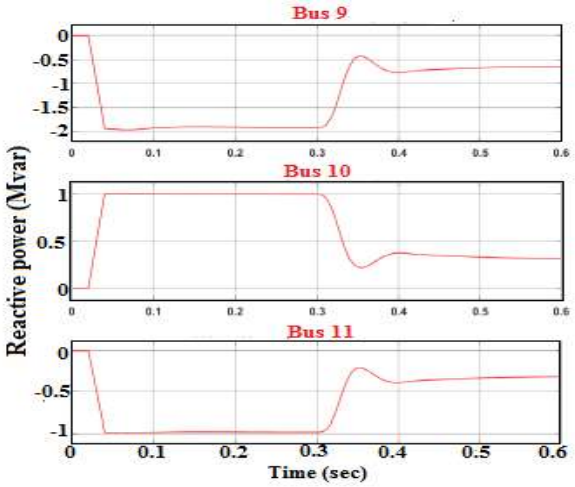

Fig. 20. Reactive power consumption of loads in islanding mode

after the islanding of the network, the voltages drop suddenly and go out of their allowed range (0.88 to 1.1). If emergency control is not performed on this MG, the system will suffer serious damage.Fig. 20 shows the reactive power consumed by loads in islanding mode.

5.3. Load Shedding

As mentioned before, the loads of each bus are divided into four equal parts, which indicate four different types of loads in terms of their importance: 1- Critical loads 2- Necessary loads 3- Important loads 4- Minor loads. Fig. 21 shows the block diagram of the loads of one of the basses.

In this paper, two different methods are used to load shedding and return the voltage to the permissible range.

A) Local Load Shedding

n this method, each bus has a local controller that measures the voltage and removes the load in order to return the voltage to the allowable range. For this purpose, a sliding surface is defined as $S = V - V_{ref}$. How to enter and exit loads using this sliding level is shown in Table 3.

If $S < -0.1$ is the first load 4, which is the least important step, is removed from the circuit. If the voltage returns to the allowable

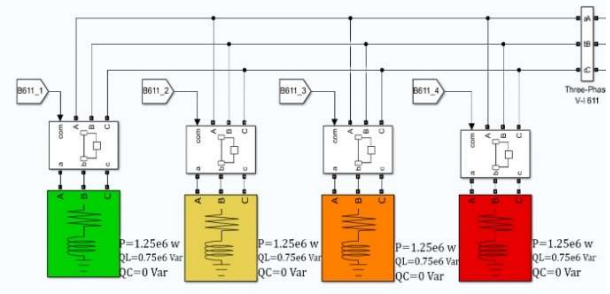

Fig. 21. Loads of bus 8

Table 3. Sliding level status and load entry and exit

Load Recycling Priority	Sliding Surface Status	Load Shedding Priority	Sliding Surface Status
L_1	$S>0.1$	L_4	$S<-0.1$
L_2		L_3	
L_3		L_2	
L_4		L_1	

range, which is equal to $-0.1<S<0.1$, the load shedding process is stopped. Otherwise, load number 3 will also be removed. It should be noted that if the line impedance is close to zero, it is practically equivalent to the parallel connection of all loads and sources together, and this method is not efficient. In this method, each controller independently removes the load, so due to the fact that after becoming islanded a severe voltage drop occurs in all the bus, all controllers are excited simultaneously and they act. In the first step, all the controllers cut off the minor loads, then measure the voltage again, and since the voltage has not returned to the allowable range, the controllers remove the second part of the load, the important loads. Since the voltage returns to the permissible range by removing two steps from the load, there is no need to continue load shedding and the controller stops. The results of this method are shown in Fig. 22 and Fig. 23. The switching state of the loads is shown in Fig. 24.

B) Central Load Shedding

In this method, the voltage of each bus is measured and sent to the central controller, and the central controller sends load shedding command signals to the breakers of each bus. The sliding level $S = V - V_{ref}$ is defined again and the priority of loads is the same as shown in Table 3, except that in this method, in addition to prioritizing loads, the buses Are also prioritized and this prioritization is shown in Table 4. In this method, after islanding, when the voltage goes out of normal operation, the least important load is removed from the least important bus. Then all voltages are measured again and sent to the central controller to stop the load shedding process if the voltage returns to the allowable range, and if the voltages do not return, this process continues until the voltage return to the allowed range.

As shown in Fig. 25 the voltage has returned to the allowable range, but it is lower than the voltage after local load shedding shown in Fig. 26. The reason for this low voltage is that the two steps in central load shedding have not been removed. So that, in this method 12 steps out of 28 steps have been removed, which two steps less than the 14 steps in local load shedding .Comparing

Table 4. Buses Priority

Buses priority from low to high	8	9	3	2	10	11	5

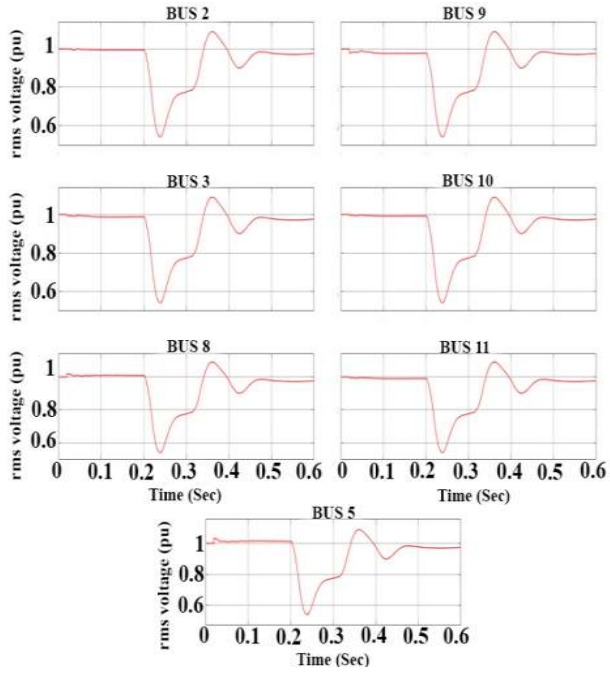

Fig. 22. Loads voltage after islanding and local load shedding

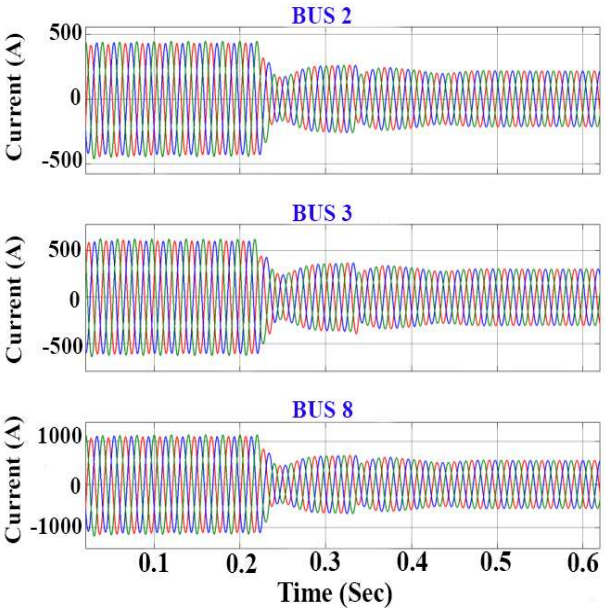

Fig. 23. Loads current after islanding and local load shedding

the two methods used to remove the load, it is found that using local load shedding, the voltage stability time (approximately 0.3 seconds) is less than the central load shedding method (approximately 1.2 seconds), but in the central load-shedding method more loads are fed. This increase in reliability is useful as long as it does not lead to voltage collapse. In the local load-shedding, there is no need to transmit the measurement signals to the central controller, but in the central load-shedding, telecommunication equipment must be used to send these signals. The following figure shows the buses voltages in both local and central load shedding modes.

In the present simulation, in order to return the voltage to the

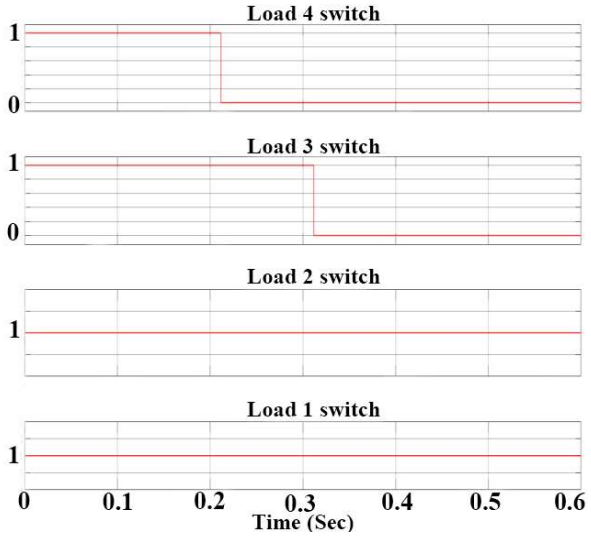

Fig. 24. The switching state of the loads during local load shedding

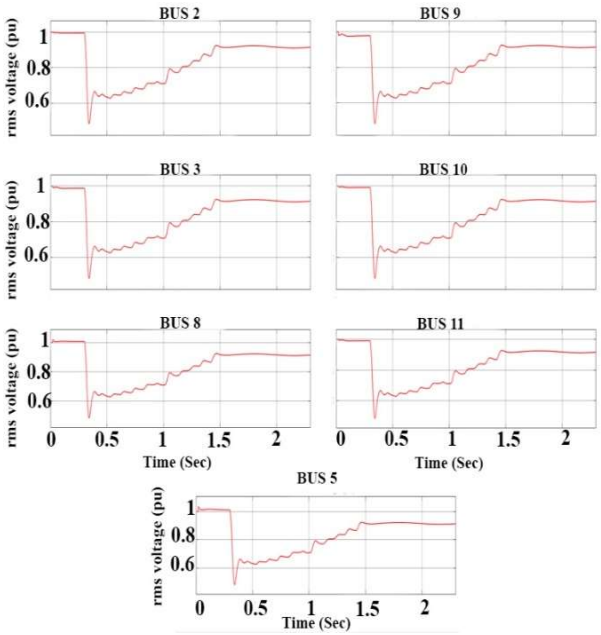

Fig. 25. Loads voltage after islanding and central load shedding

normal range, first all the less important loads were removed, and then the important loads were removed except the loads of the two buses 5 and 11. By removing each step from the load, the voltage increases little by little until it returns to the permitted range, after the voltage returns to the permitted range, there is no need to remove the load and the process of removing the load is stopped. Fig.28 in the appendix shows how to switch loads and the time sequence of load shedding. First, the least important load of the least important bus, i.e. load number 4 is removed from bus number 8. Due to the failure of the voltage to return to the permitted range, in the next step, the least important load is removed from the next least important bus, i.e. load number 4 is removed from bus number 9. This process continues until the voltages return to the permissible range. Load number 3 of bus 10 is the last load shedding. Fig. 29 in the appendix shows the flow of loads after islanding and removing the central load shedding for

(a)

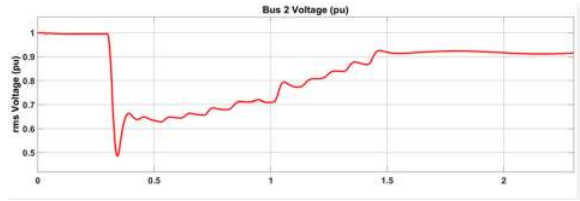

(b)

Fig. 26. Bus 2 Voltage after : (a) Local Load Shedding ; (b) Central Load Shedding

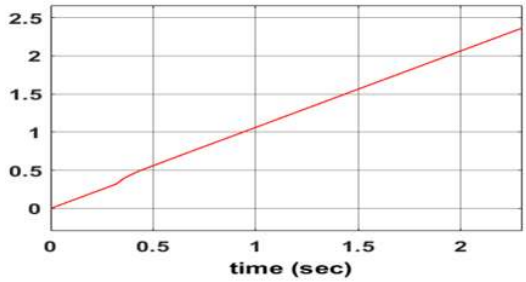

(a)

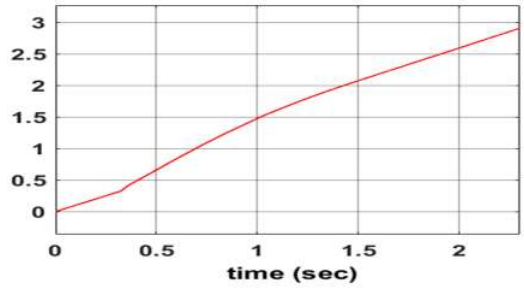

(b)

Fig. 27. ΔV^2 integral a: Local load shedding, b: Central load shedding

different busses. Another method for comparing local and central load shedding methods is to use ΔV^2 integral. Fig. 27 shows the value of this integral for two methods.

In Table 5 the values of total power removed, total power consumption and integral ΔV^2 for the two modes of local and central load shedding are compared.

To compare the two methods of local and central load shedding, we can mention these cases. In local load shedding, the total loads removed are equal to 11 MW, which was reduced to 9.75 MW in central load shedding. However, due to the higher voltage range in central load-shedding, the total power consumption in this case is 0.5 MW more than the central load-shedding. The area below the integral ΔV^2 is equal to 2.4 in local load shedding and 2.8 in central load shedding. And this shows that in central load shedding, voltage abnormality is longer than local load shedding.

Table 5. Local and central load shedding comparison

Load Shedding Mode	Total Power Removed (MW)	Total Power Consumption (MW)	ΔV^2
Local	11	11	2.4
Central	9	10.5	2.8

6. CONCLUSIONS

In this paper, the main objective was to implement SMC on DC/AC converters connected to the MG. Since MGs are growing rapidly in power systems, the need to use suitable controllers becomes more and more clear. The SMC is one of these controllers that can be used in MGs due to its resistance. By using the sliding level definition of the SMC, the controller succeeds in restoring the isolated MG voltage to the allowed range in both local and central control methods. First, the proposed MG model was checked. After modeling the microgrid and its components, they were simulated using MATLAB/SIMULINK. It was observed that the PV system and wind turbine controllers control these sources well and transfer the specified power to the microgrid. After the islanding of the micro grid and its very large voltage drop, since this voltage drop had occurred many times due to the imbalance between the output power and the demand for power consumption, the MG voltage was controlled and the power balance was established by removing the loads. Among the advantages of load removal is the maintenance and supply of important and vital loads in the islanding situation, which in the presented methods for load removal, the removal of the central load leads to the maintenance and supply of more loads.

REFERENCES

[1] V. Kumar, S.R. Mohanty, and S. Kumar, "Event trigger super twisting sliding mode control for dc micro grid with matched/unmatched disturbance observer," *IEEE Trans. Smart Grid*, vol. 11, no. 5, pp. 3837–3849, 2020.

[2] K.H. Youssef, "Microgrid reliability considering directional protection failure and optimal load shedding," *IEEE Trans. Smart Grid*, vol. 13, no. 2, pp. 877–887, 2021.

[3] G. Chen, F.L. Lewis, E.N. Feng, and Y. Song, "Distributed optimal active power control of multiple generation systems," *IEEE Trans. Ind. Electron.*, vol. 62, no. 11, pp. 7079–7090, 2015.

[4] M.R. Ghodsi, A. Tavakoli, and A. Samanfar, "A robust controller design for load frequency control in islanded microgrid clusters," *Int. Trans. Electr. Energy Syst.*, vol. 2022, 2022.

[5] G. Chen, F.L. Lewis, E.N. Feng, and Y. Song, "Distributed optimal active power control of multiple generation systems," *IEEE Trans. Ind. Electron.*, vol. 62, no. 11, pp. 7079–7090, 2015.

[6] A.B. Nassif, "A protection and grounding strategy for integrating inverter-based distributed energy resources in an isolated microgrid," *CPSS trans. power electron. appl.*, vol. 5, no. 3, pp. 242–250, 2020.

[7] H. Eskandari, M. Kiani, M. Zadehbagheri, and T. Niknam, "Optimal scheduling of storage device, renewable resources and hydrogen storage in combined heat and power microgrids in the presence plug-in hybrid electric vehicles and their charging demand," *J. Energy Storage*, vol. 50, p. 104558, 2022.

[8] S. Amirkhan, M. Radmehr, M. Rezanejad, and S. Khormali, "A robust control technique for stable operation of a dc/ac hybrid microgrid under parameters and loads variations," *Int. J. Electr. Power Energy Syst.*, vol. 117, p. 105659, 2020.

[9] T. Le and B.N. Phung, "Load shedding in microgrids with consideration of voltage quality improvement," *Eng. Appl. Sci. Res.*, vol. 11, no. 1, pp. 6680–6686, 2021.

[10] J. Peng, B. Fan, and W. Liu, "Voltage-based distributed optimal control for generation cost minimization and bounded bus voltage regulation in dc microgrids," *IEEE Trans. Smart Grid*, vol. 12, no. 1, pp. 106–116, 2020.

[11] H. Karimi and S. Jadid, "Optimal energy management for multi-microgrid considering demand response programs: A stochastic multi-objective framework," *Energy*, vol. 195, p. 116992, 2020.

[12] M. Elgamal, N. Korovkin, A.A. Menaem, and A. Elmitwally, "Day-ahead complex power scheduling in a reconfigurable hybrid-energy islanded microgrid with responsive demand considering uncertainty and different load models," *Appl. Energy*, vol. 309, p. 118416, 2022.

[13] Z. Wang, W. Wu, and B. Zhang, "A fully distributed power dispatch method for fast frequency recovery and minimal generation cost in autonomous microgrids," *IEEE Trans. Smart Grid*, vol. 7, no. 1, pp. 19–31, 2015.

[14] Y. Men, Y. Du, and X. Lu, "Distributed control framework and scalable small-signal stability analysis for dynamic microgrids," *Chin. J. Electr. Eng.*, vol. 7, no. 4, pp. 49–59, 2021.

[15] H. Farzin, M. Fotuhi-Firuzabad, and M. Moeini-Aghtaie, "Stochastic energy management of microgrids during unscheduled islanding period," *IEEE Trans. Ind. Inform.*, vol. 13, no. 3, pp. 1079–1087, 2016.

[16] Y. Jiang, Y. Yang, S.-C. Tan, and S.Y.R. Hui, "Power loss minimization of parallel-connected distributed energy resources in dc microgrids using a distributed gradient algorithm-based hierarchical control," *IEEE Trans. Smart Grid*, vol. 13, no. 6, pp. 4538–4550, 2022.

[17] J. Dong, C. Gong, H. Chen, and Z. Wang, "Secondary frequency regulation and stabilization method of islanded droop inverters based on integral leading compensator," *Energy Rep.*, vol. 8, pp. 1718–1730, 2022.

[18] C. Zhang, X. Dou, L. Wang, Y. Dong, and Y. Ji, "Distributed cooperative voltage control for grid-following and grid-forming distributed generators in islanded microgrids," *IEEE Trans. Power Syst.*, vol. 38, no. 1, pp. 589–602, 2022.

[19] C. Zhang, X. Dou, L. Wang, Y. Dong, and Y. Ji, "Distributed cooperative voltage control for grid-following and grid-forming distributed generators in islanded microgrids," *IEEE Trans. Power Syst.*, vol. 38, no. 1, pp. 589–602, 2022.

[20] T. John and S. Ping Lam, "Voltage and frequency control during microgrid islanding in a multi-area multi-microgrid system," *IET Gener. Transm. Distrib.*, vol. 11, no. 6, pp. 1502–1512, 2017.

[21] L. Zhou and J. Wu, "Magnetic levitation technology for precision motion systems: A review and future perspectives," *Int. J. Autom. Technol.*, vol. 16, no. 4, pp. 386–402, 2022.

[22] M. Zhai, Z. Long, and X. Li, "A new strategy for improving the tracking performance of magnetic levitation system in maglev train," *Symmetry*, vol. 11, no. 8, p. 1053, 2019.

[23] A. Aillane, K. Dahech, A. Chouder, T. Damak, A. Cherifi, and J. Hmad, "Control of a three-phase grid-connected inverter based on super-twisting sliding mode algorithm," in *2022 19th International Multi-Conference on Systems, Signals & Devices (SSD)*, pp. 1186–1192, IEEE, 2022.

[24] A. Samarat, B. Mehta, and S. Joshi, "Analysis and modeling of ac and dc micro-grids for prosumer based implementation," *J. Oper. Autom. Power Eng.*, vol. 9, no. 2, pp. 116–122, 2021.

[25] M.S. AlDavood, A. Mehbodniya, J.L. Webber, M. Ensaf, and M. Azimian, "Robust optimization-based optimal operation of islanded microgrid considering demand response," *Sustainability*, vol. 14, no. 21, p. 14194, 2022.

[26] E. Samsuria, Y.M. Sam, and F. Hassan, "Enhanced sliding mode control for a nonlinear active suspension full car model," *Int. J. Robot. Control Syst.*, vol. 1, no. 4, pp. 501–522, 2021.

[27] S. Ge, R. Zhao, W. Li, J. Li, Y. Liu, and Z. Wang, "Sliding-mode control for coal shearer drum height adjustment based on variable speed reaching law," *J. Vibroengineering*, vol. 22, no. 8, pp. 1782–1797, 2020.

[28] M. Zadehbagheri, M.J. Kiani, T. Sutikno, and R.A. Moghadam, "Design of a new backstepping controller for control of microgrid sources inverter.," *Int. J. Electr. Comput. Eng. (2088-8708)*, vol. 12, no. 4, 2022.

[29] M.F. Zia, E. Elbouchikhi, and M. Benbouzid, "Microgrids energy management systems: A critical review on methods, solutions, and prospects," *Appl. Energy*, vol. 222, pp. 1033–1055, 2018.

[30] O. Kohansal, M. Zadehbagheri, M.J. Kiani, and S. Nejatian, "Participation of grid-connected energy hubs and energy distribution companies in the day-ahead energy wholesale and retail markets constrained to network operation indices," *Int. Trans. Electr. Energy Syst.*, vol. 2022, 2022.

[31] E. Faraji, A.R. Abbasi, S. Nejatian, M. Zadehbagheri, and H. Parvin, "Probabilistic planning of the active and reactive power sources constrained to securable-reliable operation in reconfigurable smart distribution networks," *Electr. Power Syst. Res.*, vol. 199, p. 107457, 2021.

[32] F. Shavakhi Zavareh, E. Rokrok, J. Soltani, and M. Shahkarami, "Adaptive sliding mode control of multi-dg, multi-bus grid-connected microgrid," *J. Oper. Autom. Power Eng.*, vol. 7, no. 1, pp. 65–77, 2019.

[33] N. Abjadi, "Nonsingular terminal sliding mode control for islanded inverter-based microgrids," *J. Oper. Autom. Power Eng.*, vol. 12, no. 1, pp. 26–34, 2023.

[34] C. Wang, S. Chu, Y. Ying, A. Wang, R. Chen, H. Xu, and B. Zhu, "Underfrequency load shedding scheme for islanded microgrids considering objective and subjective weight of loads," *IEEE Trans. Smart Grid*, vol. 14, no. 2, pp. 899–913, 2022.

[35] G. Liu, T.B. Ollis, M.F. Ferrari, A. Sundararajan, and K. Tomsovic, "Robust scheduling of networked microgrids for economics and resilience improvement," *Energies*, vol. 15, no. 6, p. 2249, 2022.

[36] P. Pourghasem, H. Seyedi, and K. Zare, "A new optimal under-voltage load shedding scheme for voltage collapse prevention in a multi-microgrid system," *Electr. Power Syst. Res.*, vol. 203, p. 107629, 2022.

[37] M. Raeispour, H. Atrianfar, H.R. Baghaee, and G.B. Gharehpetian, "Robust sliding mode and mixed H_2/H_∞ output feedback primary control of ac microgrids," *IEEE Syst. J.*, vol. 15, no. 2, pp. 2420–2431, 2020.

[38] T. Madiba, R. Bansal, N. Mbungu, M. Bettayeb, R. Naidoo, and M. Siti, "Under-frequency load shedding of microgrid systems: a review," *Int. J. Model. Simul.*, vol. 42, no. 4, pp. 653–679, 2022.

[39] S.K. Jha, D. Kumar, and M. Lehtonen, "Modified vi droop based adaptive vector control scheme for demand side management in a stand-alone microgrid," *Int. J. Electr. Power Energy Syst.*, vol. 130, p. 106950, 2021.

[40] M. Azimian, V. Amir, R. Habibifar, and H. Golmohamadi, "Probabilistic optimization of networked multi-carrier microgrids to enhance resilience leveraging demand response programs," *Sustainability*, vol. 13, no. 11, p. 5792, 2021.

[41] Y. Liu, H. Wang, and C. Hou, "Sliding-mode control design for nonlinear systems using probability density function shaping," *IEEE Trans. Neural Netw. Learn. Syst.*, vol. 25, no. 2, pp. 332–343, 2013.

[42] I. Kumarswamy, T.K. Sandipamu, and V. Prasanth, "Analysis of islanding detection in distributed generation using fuzzy logic technique," in *2013 7th Asia Modelling Symposium*, pp. 3–7, IEEE, 2013.

[43] R. Carli, G. Cavone, T. Pippia, B. De Schutter, and M. Dotoli, "Robust optimal control for demand side management of multi-carrier microgrids," *IEEE Trans. Autom. Sci. Eng.*, vol. 19, no. 3, pp. 1338–1351, 2022.

Appendix A

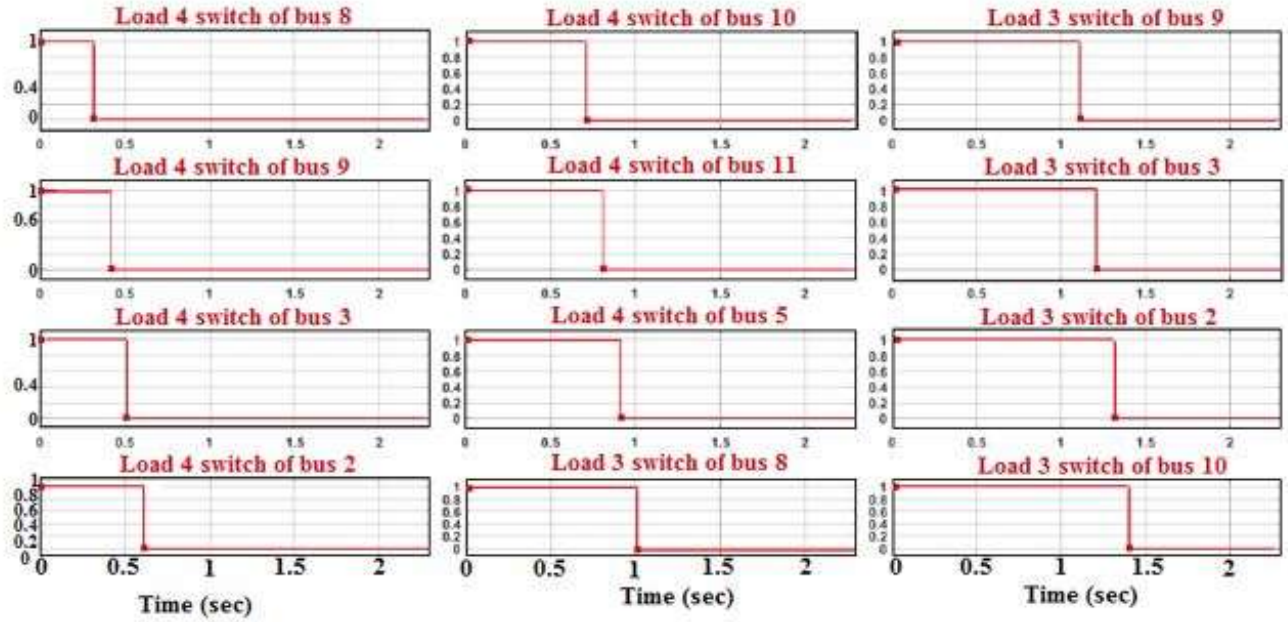

Fig. 28. Central load shedding switching status

Appendix B

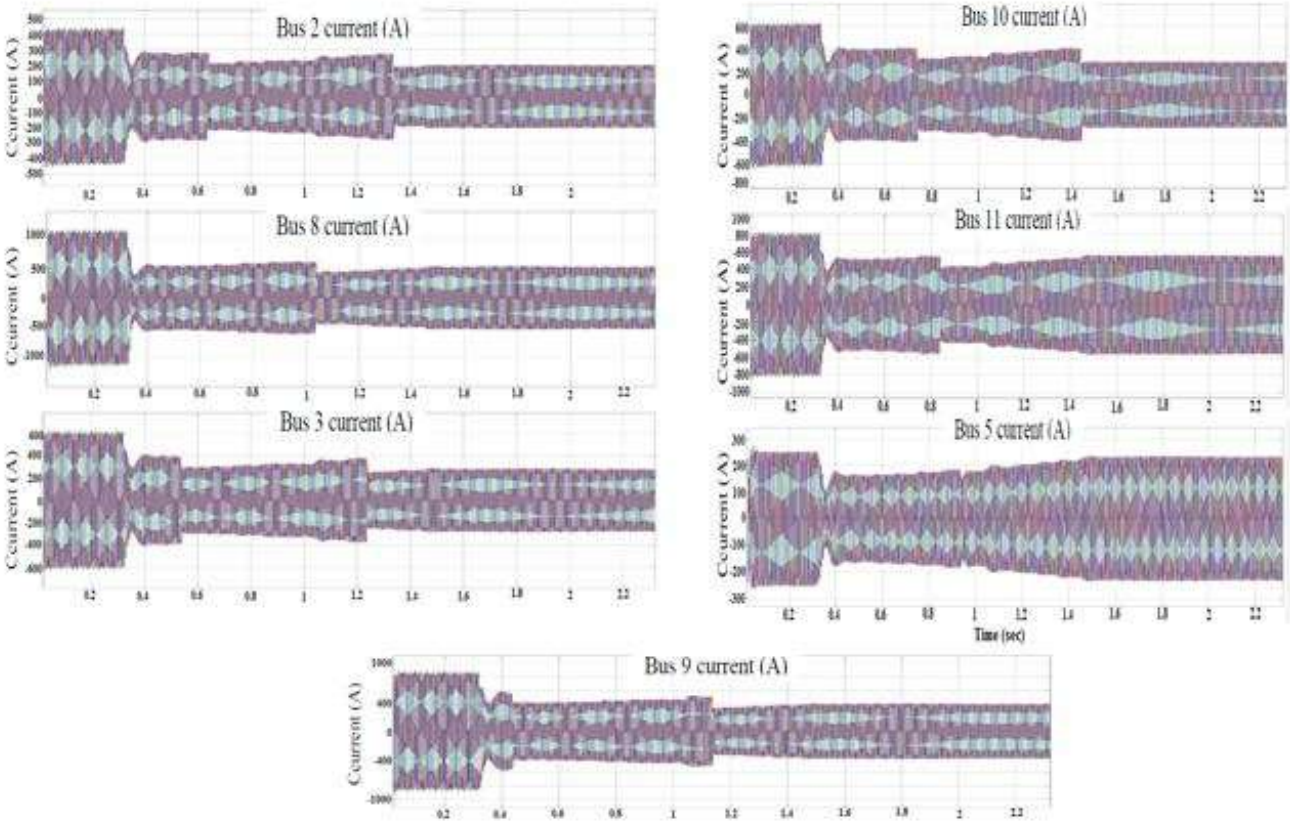

Fig. 29. Flow of loads after islanding and removal of Central load shedding